3D FINITE ELEMENT MODELING OF AIRCRAFT STRUCTURAL JOINTS WITH MULTIPLE SITE DAMAGE

J. Edward Ingram,* Young S. Kwon,* and Scott A. Fawaz†

Existing stress intensity (*K*) solutions for cracks in multiple fastener joints, such as fuselage skin splices and wing chord-wise joints, typically have not accounted for fastener force redistribution as a lead crack extends from one fastener hole to the next. The relatively recent problem of widespread fatigue damage in aging aircraft increases the need for improved K solutions which can account for multiple interacting cracks within a fastener row – i.e., multiple site damage (MSD).

Detailed solid element models were developed, using parameterized modeling techniques, to calculate the fastener forces and stress intensity factors in bolted joints containing multiple cracks. The models are full three dimensional representations of the fasteners and attached sheets. The stress intensity solutions for the lead and MSD cracks were obtained using a 3D Virtual Crack Closure Technique (3DVCCT).

An engineering model was developed from the finite element solutions to calculate the stress intensity solutions for multiple cracks, and predict the link-up of the multiple cracks and residual strength of the joint.

DEVELOPMENT OF CRACKED BOLTED JOINT MODELS

A series of solid element models were developed to simulate typical aircraft bolted joint configurations, which are considered to be susceptible to widespread fatigue damage (WFD). For fuselage structure, this would include longitudinal and circumferential skin splices, and for wing structure, chord-wise joints and rib attachment locations. The models were developed in a parametric language to facilitate re-meshing of the models to analyze varying joint dimensions and multiple crack configurations. The Lockheed Martin finite element code, DIAL, was selected due its capability for parameterized input as well as its 'interface element' for simulating contact (fastener bearing) behavior.

Three configurations of the cracked bolted joints were modeled. 1) two-row single shear, 2) three-row single shear, and 3) two row double shear joints. Twenty node parabolic solid elements were used to represent the skin panels and fasteners in all three configurations. The interface element, which was used at all fastener bearing areas and skin contact areas, is a two-dimensional, eight-node element, with normal and shear stress capability. For the models described here, the shear stress capability was not used (i.e, frictionless sliding was assumed at all contact surfaces). Figure 1 shows a typical configuration of the bolted joint models, including a typical mesh detail of the region near a cracked fastener hole. The shapes of the part-through cracks, such as the one in the detail of Figure 1, are set up to be variables in the parameterized models.

A 3D Virtual Crack Closure Technique (3DVCCT) was used to calculate the stress

* Lockheed Martin Aeronautics Company, 86 South Cobb Dr., Marietta, GA. 30063-0670

† United States Air Force Academy, HQ USAFA/DFEM, 2354 Fairchild Drive, Fairchild Hall Suite 6L-155, USAF Academy, CO 80840-6420

intensity along the crack front. This version of the virtual crack closure method uses forces at nodes "ahead of" the crack front (the un-cracked region), and displacements "behind" the crack front (in the crack wake) to calculate the strain energy release rate with a single execution of the model. The essentials of the method are illustrated in Figure 2. More thorough treatment of the 3DVCCT methods was given by Shivakumar, Tan, and Newman [1] and Fawaz [2]. The single execution (as opposed to solving once for forces and again for displacements at the same nodes) was particularly important in this study, as the nonlinear solution of the large (>200,000 degrees of freedom) models required days to complete, and well over 100 variations of the parametric models were run.

The requirement for nonlinear solution of the models stemmed from the contact behavior at the bearing surfaces and from the secondary bending due to eccentric load paths. A far-field or remote load corresponding to a stress of 10 ksi was selected as the target load for each run. This value was reasonable from the standpoint of typical operational loading at these aircraft joints.

Once the K at each point along the crack front was calculated, the normalized stress intensity, F, is:

$$F = \frac{K}{S\sqrt{\frac{\pi a}{Q}}} \tag{1}$$

Where S is the remote stress, and Q is the crack shape parameter, computed as follows:

$$Q = 1 + 1.464\left(\frac{a}{c}\right)^{1.65} \quad for \quad \frac{a}{c} \le 1 \qquad and \qquad Q = 1 + 1.464\left(\frac{c}{a}\right)^{1.65} \quad for \quad \frac{a}{c} \ge 1$$

For through-cracks, the normalized stress intensity is:

$$F = \frac{K}{S\sqrt{\pi a}} \tag{2}$$

where K is obtained at several points along the crack front (through the plate thickness), just as in the part-through configuration.

Before attempting to run the parameter study of various crack shapes and sizes, several sensitivity studies were conducted to establish the model mesh requirements for solution accuracy. Well known stress intensity solutions for part-through cracks from open holes and from single-edge notched tension (SENT) specimens were available from Zhao et. al.[3,4]. DIAL models of these crack configurations were created and studied for the effect of mesh imperfection on accuracy. Once it was established that the DIAL models with obviously acceptable mesh refinement and regularity (no high element aspect ratios or skewed elements) agreed with these known solutions (comparison is shown in Figure 3), various mesh imperfections were studied. The following requirements, regarding the elements in the fine-mesh region (the "crack band") near the crack front, were derived from these studies:

1. There should be three rows of identical solids ahead of and behind the crack front (in the high stress gradient region).
2. Element aspect ratios for the 20 node parabolic solids should not exceed 10 (provided the requirements of 1 are met).

3. Element skew (trapezoidal shape) should not exceed 30 degrees (angles formed by two adjacent element faces should be within 30 degrees of orthogonal).

After establishing the mesh requirements and incorporating them into the DIAL parametric language, 13 separate model configurations were created. These included: 2-row and 3-row single shear joints, 2-row double-shear (butt joints), 1, 3 and 5 ligaments failed, through and part-through crack shapes. Additionally, separate models were needed for calculating *K* at the lead crack and at the MSD crack.

Figure 4 is a graphical representation of the K solution obtained from a typical model execution. This particular plot shows F along the crack front for the case of three ligaments cracked in a two-row, single shear splice. In this case, the lead crack is emerging from the fastener hole as a part-through crack (with $a_1/c_1=1$) at various sizes. The MSD cracks are also part-through, with $a_2=c_2=0.035$ inch.

Figure 5(a) shows a typical distribution of the fastener forces, calculated from one of the DIAL runs, for a two-row splice with the crack configuration shown in the figure. The fastener forces were calculated by summing the contact forces on the interface elements located between the solid elements of the fastener shank and the hole. The bar chart shows the expected trend of larger cracks causing reduced local stiffness and reduced fastener forces. The load shedding in the crack path is accompanied by shifting some of the load to fasteners ahead of the lead crack in addition to some load being transferred to the un-cracked row. Distributions such as this were calculated for each model and crack configuration. Figure 5(b) shows the peaking and shedding behavior of the forces at four MSD-cracked fastener holes as the crack extends. Also shown in the figure is an engineering model, developed from the DIAL results, that approximates the model-calculated force redistribution. In an un-cracked skin splice, the fastener forces in a given row can be calculated from the remote loading, N_x, percent load transfer, PLT, and fastener spacing, S:

$$P_f = N_x S(PLT) \tag{3}$$

From the DIAL results can be seen an increase in the fastener forces ahead of a crack in some proportion to the lead crack length. It was assumed that the peak value of the fastener force, just at the instant prior to a lead crack extending into (or "absorbing") the next MSD crack, is related to local stress in the region just ahead of the crack tip. This local stress is proportional to the square root of the crack length; or, in this case, the distance from the center of the lead crack to the fastener. Therefore the term $\sqrt{x_i}$ was added to equation (3). After comparing to the DIAL-calculated forces, a correction term, involving the natural log of the fastener distance, x_i, was included to improve agreement with the DIAL. The final equation used in the engineering model to approximate the peak fastener force is:

$$P_f = N_x S(PLT)\sqrt{x_i}\left[-0.118\ln(x_i)+0.915\right] \tag{4}$$

Once the peak values are determined, the reduction of the fastener force as the lead crack extends past the fastener hole is observed to fit a decay function:

$$P_f(c_1) = P_{next}\ln(-1.3c_1) \tag{5}$$

As with the peak values, this relationship for load-shedding behavior is determined by simply fitting the decay function to the DIAL results. The purpose of developing equations that relate fastener force to crack length is to create an engineering model for stress

intensity solutions. When the fastener forces are determined using equations (4) and (5), the stress intensity can be calculated by superposition of known solutions for the following crack configurations:

- Cracks emerging from slots (Paris and Tada [5])
- Cracks with point forces (the fastener forces) on the crack flanks (Wu and Carlsson [6])
- Interaction of adjacent cracks (Kamei and Yokiburi [7])
- Finite width effects (Isida [8])

These solutions were combined to create the engineering model for cracks in bolted joints. The result of this process is shown in Figure 6, in which the engineering model is compared to the DIAL-calculated *K* solutions for the two-row splice with 0.05 inch MSD cracks. The standard solution for cracks emerging from and extending into open holes is also shown for comparison to the engineering model. The stress intensity values calculated from the DIAL FEM and from the engineering model exceed the open hole solution for all crack lengths, due to the load transfer at the holes.

Predicting Link-up of Lead Cracks and MSD Cracks

The primary purpose for developing the 3D models was to improve the capability to predict residual strength of aircraft joints with MSD. Prior to this effort, several researchers (Broek [9], Ingram, [10], Smith [11]) investigated a method for predicting the link-up of multiple cracks in ductile alloys. All based their models on the theory that when the plastic zones at two adjacent crack tips touch (i.e., the entire distance between two crack tips has yielded) failure of that ligament will occur. This method, which is based on linear elastic fracture mechanics methods for calculating the stress intensity, and subsequently the plastic zone sizes, was determined by each researcher to be a fairly reliable predictor of link-up of cracks from open holes or line cracks. Thus, our hypothesis was that if the stress intensity solutions were available for bolted joints with multiple cracks, then perhaps the residual strength of aircraft skin splices could be predicted with equal accuracy.

The engineering model, developed from the DIAL analyses described earlier, together with the plastic zone touch link-up method were incorporated into a computer program to predict the residual strength of MSD-cracked skin splices. Input to this program consists of the material yield strength, the fastener diameters, spacing, MSD crack sizes and percentage of far-field load in the critical row of a splice. The program uses the joint geometry and the mechanical properties to predict the far field stress level at which crack link-up (and therefore lead crack extension) and joint failure will occur.

The residual strength computer program was used to analyze MSD-cracked bolted joint specimens, which were tested at the Air Force Research Laboratories in Dayton, Ohio. In his report describing these tests, Shrage [12] provides the joint configuration, initial crack lengths, loads at first link-up, and maximum test load for each of four specimens which represent typical aircraft skin splices. All of the test specimens were fitted with anti-buckling guides to prevent buckling of the crack faces as well as provide constraint against secondary bending. Constraint of the secondary bending was not desired, but an artifact of preventing crack face bulging. Table 1 gives a summary of the test specimen configurations, link-up and maximum panel loads, and calculations from the DIAL model-based residual strength program.

TABLE 1 Summary of AFRL MSD Test Results [12] and Comparison to Calculated Values

Test ID MSD -	Fast. Spac. (inch)	Fast. Dia. (inch)	Crack Half Length a_{msd} (inch)	Crack Half Length a_1 (inch)	Crack Half Length $a_{1\text{-local}}$ (inch)	Ligament (inch)	Test Event	Test Stress (ksi)	Calculated 2D Models (ksi)	% Error 2D	Calculated 3D Models (ksi)	% Error 3D
1-2	1.5	5/32	0.05	6.950	0.872	0.422	1st Link-up	14.90	13.54	-9.13	12.11	-18.72
			0.05	7.628	0.050	1.244	Max Load	17.20	18.00	4.65	18.08	5.10
1-3			0.10	6.950	0.872	0.372	1st Link-up	12.52	12.69	1.36	11.51	-8.04
			0.10	7.678	0.100	1.144	Max Load	17.42	17.44	0.11	17.51	0.52
501-2	1.14	3/16	0.05	6.410	0.616	0.286	1st Link-up	13.23	12.06	-8.84	11.41	-13.77
			0.05	6.984	0.050	0.853	Max Load	17.97	16.68	-7.18	16.78	-6.62
501-3			0.10	6.410	0.616	0.236	1st Link-up	11.24	10.80	-3.93	9.76	-13.21
			0.10	7.034	0.100	0.753	Max Load	14.90	15.79	5.97	15.87	6.50
503-2	1.6	3/16	0.05	7.400	0.906	0.456	1st Link-up	14.29	13.13	-8.09	12.66	-11.41
			0.05	8.144	0.050	1.313	Max Load	18.31	17.39	-5.04	17.39	-5.00
503-3			0.10	7.400	0.906	0.406	1st Link-up	12.24	12.31	0.60	11.39	-6.98
			0.10	8.194	0.100	1.213	Max Load	16.62	16.59	-0.17	16.46	-0.99
505-2	1.5	5/32	0.05	6.950	0.872	0.422	1st Link-up	15.43	13.77	-10.75	13.03	-15.58
			0.05	7.628	0.050	1.244	Max Load	19.69	18.23	-7.41	18.38	-6.65
505-3			0.10	6.950	0.872	0.372	1st Link-up	13.70	12.90	-5.81	11.70	-14.58
			0.10	7.678	0.100	1.144	Max Load	18.44	17.77	-3.66	17.84	-3.28

The residual strength program developed from the 3D DIAL models generally under-predicts the first link-up event as well as the maximum test load. The average percent error between the calculated and test values for all events (first link-up and failure) is 8.6 percent. However, if failure loads only are considered, the agreement between analysis and test is better, with an average error of 4.3 percent. This is well within the ranges obtained in the open hole and slit-crack comparisons.

The anti-buckling guides used in the test not only constrain secondary bending but also crack face bulging (buckling). These phenomena occur in aircraft joints; therefore, anti-buckling guides were not considered in the 3D models. Both secondary bending and crack face bulging lead to lower residual strength values because the local stresses are higher than those when anti-buckling guides are used. This difference is thought to account for the difference between analysis and test. Note from Table 1 that the original 2D model calculations (which do not account for secondary bending or crack face bulging) agree more closely for first link-up than the 3D models. In each test panel, the length of the "installed" lead crack is such that the local crack length (i.e., the distance from the previous fastener hole to the tip of the lead crack) is considerably larger than for each subsequent link-up. It is believed that for these cases, the effects of local secondary bending, that are present in the model but prevented in the test panels, are greatest; and therefore, the differences between analysis and test are also greatest.

Lessons Learned

Obtaining converged solutions at the target load proved extremely difficult for the models with larger lead cracks (three and five ligaments cracked). Large displacements at the fastener/interface element/skin contact area, which resulted from the combined effects of the eccentric load path and large cracks, are suspected to be the main source of the numerical difficulty.

REFERENCE LIST

(1) Shivakumar, K.N., Tan, P.W., and Newman, J.C., Jr., "A Virtual Crack Closure Technique for Calculating Stress Intensity Factors for Cracked Three Dimensional Bodies", *International Journal of Fracture* 36: R43-R50, 1988.

(2) Fawaz, S. A., "Fatigue Crack Growth in Riveted Joints," Ph.D. Dissertation, Delft University Press, 1997.

(3) Zhao, W., Newman, J. C., Jr., Sutton, M. A., Wu, X. R. and Shivakumar, K. N.,"Analysis of Corner Cracks at a Hole by a 3-D Weight Function Method with Stresses from Finite Element Method," *NASA TM-110144*, July 1995.

(4) Zhao, W., and Newman, J. C., Jr., "Modification of Stress Intensity Factor Equation for Corner Crack from a Hole Under Remote Bending," April 1996.

(5) Paris, P.C., and Tada, H., "The Stress Analysis of Cracks Handbook," Del Research Corp., 1973.

(6) Wu, X. R., and Carlsson, A. J., "Weight Functions and Stress Intensity Factor Solutions", Pergamon Press, 1991.

(7) Kamei, A., and Yoloburi, T., "Two Collinear Asymmetrical Elastic Cracks," Report of the Research Institute for Strength and Fracture of Materials, Tohoku University, Vol. 10, Section 1-4, pp. 41-42, December 1974.

(8) Isida, M., "Stress Intensity Factors for the Tension of an Eccentrically Cracked Strip," *Journal of Applied Mechanics* Series E, September 1966, p. 674-675.

(9) Broek, D., "The Effects of Multi-Site Damage on the Arrest Capability of Aircraft Fuselage Structures," FractuResearch TR 9302, June, 1993.

(10) Ingram, J.E., Y. S. Kwon, K. J. Duffié and W. D. Irby , "Residual Strength Analysis of Aircraft Skin Splices with Multiple Site Damage," Proceedings of *the 2nd Annual NASA/FAA/DOD Conference on Aging Aircraft*, Williamsburg, VA., Aug. 31-Sept. 3, 1998.

(11) Smith, B., Movak, A., Saville, P., Myose, R., and Horn, W., "Improved Engineering Methods for Determining the Critical Strengths of Aluminum Panels with Multiple Site Damage in Aging Aircraft," Proceedings of *the 2nd Annual NASA/FAA/DOD Conference on Aging Aircraft*, Williamsburg, VA., Aug. 31-Sept. 3, 1998.

(12) Shrage, D. B., "Multiple Site Damage in Flat Panel Testing," Final Report for Period of 13 May 1999 – 08 December 1999, AFRL-VA-WP-TR-2001-3005, October 2000.

Figures

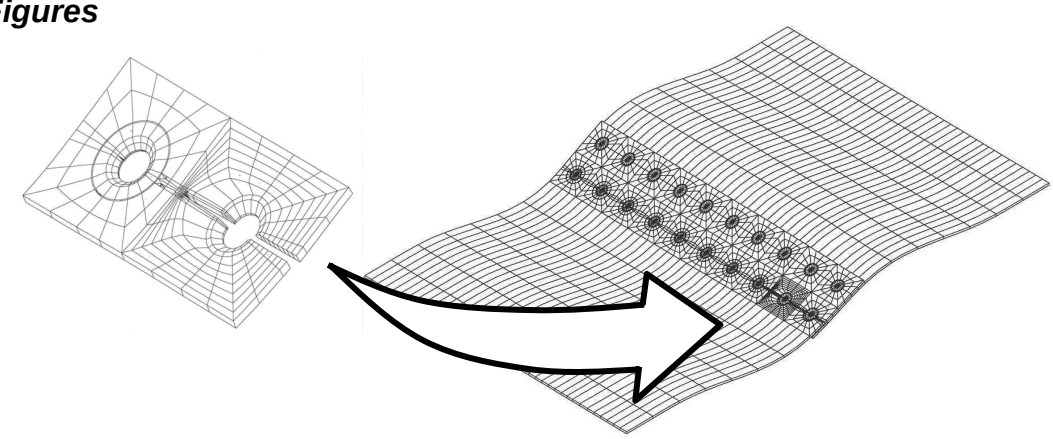

Figure 1 Two-row lap splice model, shown in displaced shape (displacements magnified). Inset shows detail at lead crack tip.

$$G_i = \frac{1}{2\Delta w_i}\sum_{j=1}^{5} C_j F_j V_j$$

$$C_1 = C_2 = \frac{w_i}{w_{i-1} + w_i}$$

$$C_3 = 1$$

$$C_4 = C_5 = \frac{w_i}{w_i + w_{i+1}}$$

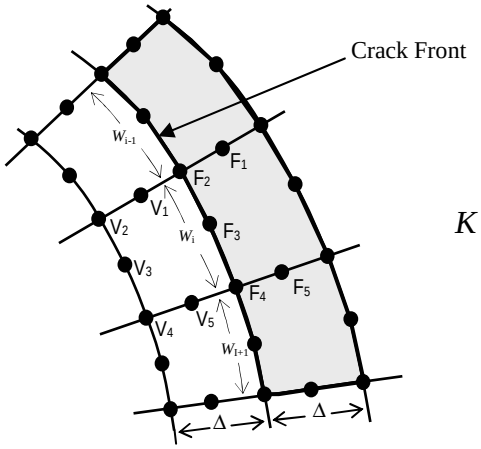

$$K = \sqrt{\frac{GE}{1-\nu^2}}$$

Figure 2 Illustration of 3DVCCT strain energy release rate calculations from grid point forces

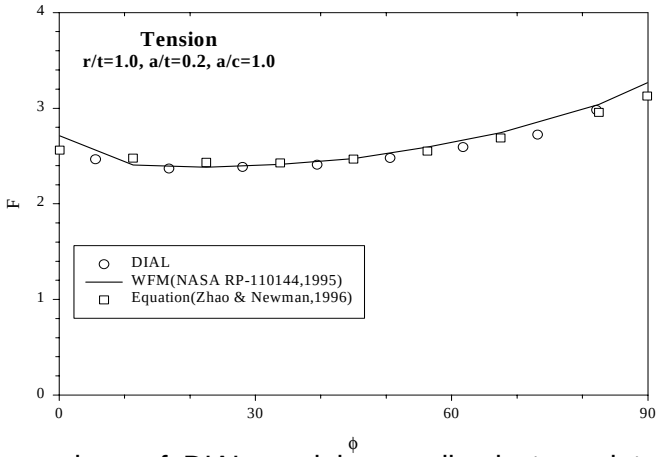

Figure 3 Comparison of DIAL model normalized stress intensity, F, to existing solutions from Zhao and Newman [3,4]

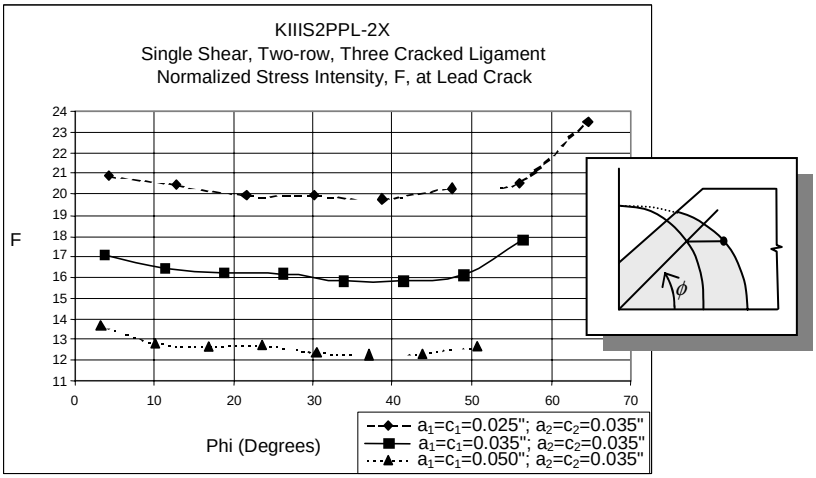

Figure 4 Normalized stress intensity along quarter-circular crack front at loaded fastener hole for three crack sizes

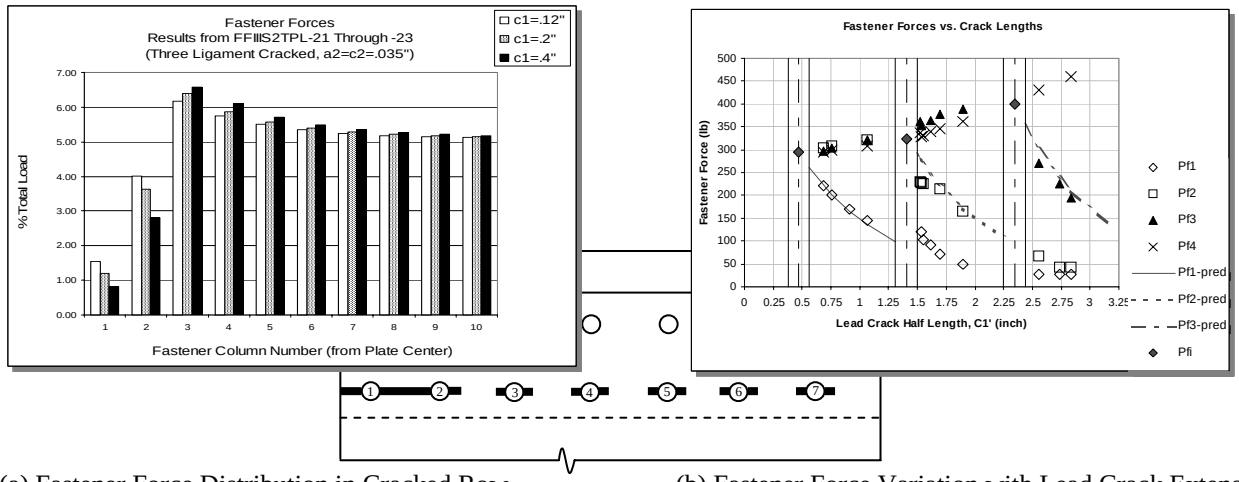

(a) Fastener Force Distribution in Cracked Row (b) Fastener Force Variation with Lead Crack Extension

Figure 5 Distribution of fastener forces from DIAL 3D models and comparison to engineering model

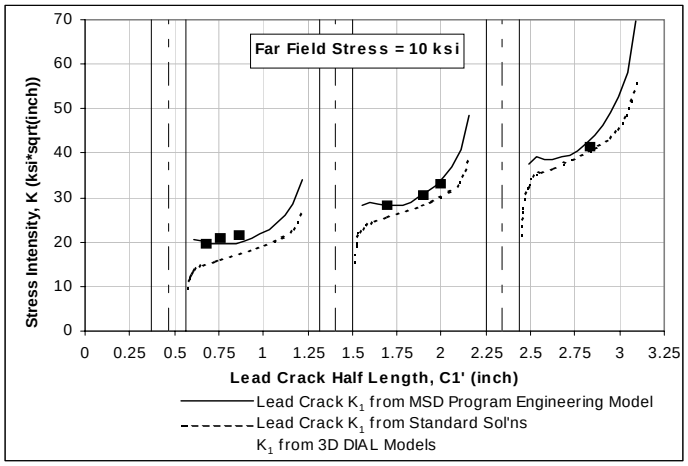

Figure 6 Comparison of stress intensity solutions from 3D DIAL models, engineering approximation and standard solutions